Vglut1 and ZnT3 co-targeting mechanisms regulate vesicular zinc stores in PC12 cells

Gloria Salazar, Branch Craige, Rachal Love, Daniel Kalman and Victor Faundez*

Department of Cell Biology, Center for Neurodegenerative Disease, and Department of Pathology and Laboratory Medicine, Emory University, 615 Michael Street, Room 446, Atlanta, GA 30322, USA

*Author for correspondence (e-mail: faundez@cellbio.emory.edu)

Accepted 11 February 2005
Journal of Cell Science 118, 1911-1921 Published by The Company of Biologists 2005
doi:10.1242/jcs.02319

Summary

The lumenal ionic content of an organelle is determined by its complement of channels and transporters. These proteins reach their resident organelles by adaptor-dependent mechanisms. This concept is illustrated in AP-3 deficiencies, in which synaptic vesicle zinc is depleted because the synaptic-vesicle-specific zinc transporter 3 does not reach synaptic vesicles. However, whether zinc transporter 3 is the only membrane protein defining synaptic-vesicle zinc content remains unknown. To address this question, we examined whether zinc transporter 3 and the vesicular glutamate transporter Vglut1 (a transporter that coexists with zinc transporter 3 in brain nerve terminals) were co-targeted to synaptic-like microvesicle fractions in PC12 cells. Deconvolution microscopy and subcellular fractionation demonstrated that these two transporters were present on the same vesicles in PC12 cells. Vglut1 content in synaptic-like microvesicle fractions and brain synaptic vesicles was partially sensitive to pharmacological and genetic perturbation of AP-3 function. Whole-cell flow-cytometry analysis of PC12 cell lines expressing zinc transporter 3, Vglut1 or both showed that vesicular zinc uptake was increased by Vglut1 expression. Conversely, production of zinc transporter 3 increased the vesicular uptake of glutamate in a zinc-dependent fashion. Our results suggest that the coupling of zinc transporter 3 and Vglut1 transport mechanisms regulates neurotransmitter content in secretory vesicles.

Key words: Zinc, Vglut1, ZnT3, Synaptic vesicle, AP-3.

Introduction

Membrane proteins present in a vesicle define the lumenal content of small-molecule mediators such as ions and amino acids. This is particularly important in secretory vesicles, like synaptic vesicles, in which the lumenal contents act as neurotransmitters or neuromodulators that determine target-cell responses. Thus, the mechanisms that control the membrane-protein composition of vesicles are central in defining how a vesicle acquires its lumenal content. Adaptor complexes (APs) play a fundamental role in membrane-protein traffic by regulating the packing of membrane proteins into distinct vesicle carriers (Bonifacino and Traub, 2003; Robinson, 2004). Among the adaptor complexes, AP-3 is unique because its function is altered in several vertebrate genetic deficiencies. In mice, the *mocha* allele results in a lack of AP-3 and is characterized by a profound neurological phenotype (Kantheti et al., 1998; Kantheti et al., 2003). We have determined that the mocha neurological phenotype emerges in part from defects in the assembly of synaptic vesicles. In the absence of AP-3, a synaptic-vesicle-specific zinc transporter 3, ZnT3, is absent from a synaptic-vesicle subpopulation because the vesicles containing ZnT3 are not properly assembled (Salazar et al., 2004b). As a consequence, synaptic-vesicle zinc stores are severely reduced from AP-$3^{-/-}$ brain synapses (Kantheti et al., 1998; Kantheti et al., 2003).

Ionic zinc is found ubiquitously throughout synapses of the mammalian central nervous system, where it plays fundamental roles in synaptic function and plasticity (Baranano et al., 2001; Li et al., 2001; Lu et al., 2000; Paoletti et al., 1997; Ueno et al., 2002; Vogt et al., 2000). Zinc is concentrated in presynaptic terminals, where it is stored in synaptic vesicles by a mechanism dependent on ZnT3 (Palmiter et al., 1996). ZnT3 function is an absolute requirement for the establishment of synaptic zinc pools. Deficiencies in ZnT3 are characterized by the absence of ionic zinc from brain synaptic vesicles (Cole et al., 1999) and, at the organ level, propensity to seizures (Cole et al., 2000). The roles of synaptic zinc are not just restricted to normal synaptic physiology. In fact, pathogenic amyloid peptide aggregation is triggered by ionic zinc, a process that in vivo can be ameliorated by genetic ablation of ZnT3 (Gouras and Beal, 2001; Lee et al., 2002; Weiss et al., 2000). Although ionic zinc is involved in fundamental brain processes, the mechanisms that control ZnT3-dependent zinc storage in synaptic vesicles are poorly understood.

ZnT3 protein levels are regulated by global genomic and non-genomic mechanisms. Estrogens (Lee et al., 2004), aging (Saito et al., 2000) and the adaptor complex AP-3 control the ZnT3 protein level (Kantheti et al., 1998; Salazar et al., 2004a). Mechanisms that regulate vesicular zinc transport independently of the ZnT3 level are largely unexplored. However, heterogeneity in the distribution of vesicular ionic zinc content at the single-neuron level suggests that ZnT3

could be under the control of local mechanisms affecting its transport activity (Salazar et al., 2004b). In fact, we recently reported that the availability of chloride channels in synaptic vesicles regulates vesicular zinc content (Salazar et al., 2004a). This suggests that anionic shunt mechanisms could favor zinc uptake into synaptic vesicles. Glutamate is well suited to provide an anionic shunt, because the vesicular glutamate transporter 1 Vglut1 (Bellocchio et al., 1998) is expressed with ZnT3 (Palmiter et al., 1996; Wenzel et al., 1997) in synaptic terminals that co-release zinc and glutamate (Huang, 1997; Takeda, 2000).

It is presently unknown whether the intravesicular glutamate levels can modulate the extent to which zinc is transported into the lumen of the same vesicle. Such a mechanism would require that both ZnT3 and Vglut1 coexist on the same vesicle, and share a similar targeting mechanism. In this study, we have tested these hypotheses by reconstituting ZnT3-dependent and Vglut1-dependent transport mechanisms in PC12 cells. Our results indicate that ZnT3 and a pool of Vglut1 are co-targeted to the same vesicle population and that the ZnT3 and Vglut1 transport mechanisms are reciprocally regulated. The findings presented in this study show that multiple transport mechanisms converge on the same vesicle to define their lumenal neurotransmitter content.

Materials and Methods

Cell culture and transfection

PC12 KB wild-type and cell lines producing VAMPII N49A (Faundez et al., 1997; Grote et al., 1995), Vglut1 (Vgl cells) or Vglut1 plus ZnT3 (VglZn cells) were generated and maintained as described (Salazar et al., 2004b). Vgl cells (a gift from R. Edwards, University of California, San Francisco, CA, USA) were transfected with pcDNA3.1-ZnT3, and the pEF6/V5-His plasmid encoding the blasticidin-resistance gene (Invitrogen). Double transfectant clones were selected with 10 μg ml^{-1} blasticidin and 0.8 mg ml^{-1} G418. Nerve growth factor (NGF) differentiation was performed with 50 ng ml^{-1} NGF for 4-7 days.

Antibodies and plasmids

Antibodies used were against synaptophysin (SY38, Chemicon, Temecula, CA), transferrin receptor (H68.4, Zymed, South San Francisco, CA) and VAMP II (69.1), polyclonal and monoclonal antibodies against Vglut1 (Synaptic Systems, Goettingen, Germany), and rabbit antibody against glutamate (Chemicon International). Anti-SV2 (10H4) and anti-AP-3δ (SA4) antibodies were from the Developmental Studies Hybridoma Bank (University of Iowa). ZnT3 affinity-purified antibodies, *ZnT3HA* cDNA and PC12 cells ZnT3HA clone 4 have already been described (Salazar et al., 2004b). Other anti-AP-3 antibodies were described previously (Faundez et al., 1998; Salem et al., 1998). Syntaxin-13/GFP fusion in pEGFP was a gift of A. Peden (Genetech, South San Francisco, CA).

Immunofluorescence

Cells were processed for immunofluorescence as described (Salazar et al., 2004a). Secondary antibodies conjugated with Alexa-488 were used. Fluorescence was analysed using a FACScalibur System (Becton Dickinson). Epifluorescence microscopy was performed using Leica DMR-E fluorescence microscope equipped with narrow band-pass filters and a Hammamatsu Orca camera. Images were captured and processed using Open Lab software (Improvision, Lexington, MA). Alternatively, images were acquired with a scientific-grade cooled charge-coupled device (Cool-Snap HQ with ORCA-ER chip) on a multiple-wavelength, wide-field, three-dimensional microscopy system (Intelligent Imaging Innovations, Denver, CO), based on a 200 M inverted microscope using a 63× lens with numerical aperture 1.4 (Carl Zeiss, Thornwood, NY). Immunofluorescent samples were imaged at room temperature using a Sedat filter set (Chroma Technology, Rockingham, UT), in successive 0.25-μm focal planes. Out-of-focus light was removed with a constrained iterative deconvolution algorithm (Swedlow et al., 1997). Calibrations bars correspond to 6 μm.

Cell fractionation, immunomagnetic isolations and immunoblot

PC12 cells homogenization, differential fractionation and glycerol velocity sedimentation were performed as described (Salazar et al., 2004b). Immunomagnetic isolations were done using Dynabeads M-450 (Dynal, Oslo, Norway) preincubated with monoclonal antibodies against Vglut1, the δ subunit of AP-3 or the hemagglutinin (HA) epitope. Detailed procedures are as described by Salazar et al. (Salazar et al., 2004b).

The preparation of frozen brains from mocha AP-3-deficient (*gr/gr, mh/mh*) and wild-type (*gr/gr*) mice, or wild type and *Ap3b2*$^{-/-}$ mice on a C57BL/6 (B6) genetic background has been previously described (Seong et al., 2005). Brains were pulverized to a fine powder using porcelain mortars under a continuous supply of liquid nitrogen (Salazar et al., 2004a). Extracts were thawed at 4°C in five volumes of buffer A (150 mM NaCl, 10 mM Hepes, pH 7.4, 1 mM EGTA, 0.1 mM $MgCl_2$) plus Complete™ antiprotease mixture (van de Goor et al., 1995). Homogenates were sedimented at 1000 ***g*** for 10 minutes to generate S1 supernatants. S1 supernatants were further fractionated at 27,000 ***g*** for 45 minutes to obtain high-speed supernatants, which were resolved on glycerol velocity gradients as described above.

Gradient fractions were analysed by immunoblot and immunoreactivity was revealed by enhanced chemiluminescence. The synaptic vesicle peak was defined as fractions 8-12. Immunoreactive bands were quantified using NIH Image 1.62 software (http://rsb.info.nih.gov/nih-image/download.html) (Faundez et al., 1997; Faundez and Kelly, 2000; Grote et al., 1995).

Zinquin staining and flow cytometry

Zinc uptake, staining with the zinc-selective fluoroprobe zinquin (Nasir et al., 1999; Zalewski et al., 1993), two-photon microscopy and morphometric analysis (using Metamorph software, Universal Imaging, Downingtown, PA) have been described (Salazar et al., 2004a). After zinquin staining, cells were washed at 4°C. Fluorescence was determined using a MoFlo High-performance Cell Sorter from DakoCytomation (Fort Collins, CO). The laser used for the forward and side scatter was a Coherent I-305, 488 nm argon laser. Zinquin was excited with a Coherent I-90 krypton laser set to 305 nm. The filters used were a 440 long-pass and a 450/65 in front of the photomultiplier tube. Data analysis was performed using FloJo version 4.4.4 (Treestar, Ashland, OR). To depict the data in a normalized fashion, we use % of maximum.

In vitro glutamate uptake

Vesicular glutamate uptake was performed as described (Bellocchio et al., 2000). Briefly, synaptic-like microvesicle (SLMV) fractions were obtained from PC12 S2 supernatants by centrifugation at 200,000 ***g*** for 1 hour. Membranes were resuspended in 0.32 M sucrose, 10 mM Hepes-KOH, pH 7.4, 4 mM KCl, 4 mM $MgSO_4$, 4 mM ATP. Assays were performed in the presence of 50 μM [^{3}H]-glutamate at 29°C. All the assays were performed within the linear range (5 minutes) using 100 μg membrane protein per assay. Uptake

was terminated by filtration and cold washes with 155 mM potassium tartrate and 10 mM HEPES, pH 7.4.

Glutamate staining

PC12 cells were loaded with 25 μM $ZnSO_4$ and 1 mM glutamate in Dulbecco's modified Eagle's medium (DMEM) for 1 hour at 37°C, washed three times with PBS followed by centrifugation for 5 minutes at 95 ***g***. Cells were resuspended in 1 ml 1% glutaraldehyde, 2.5% paraformaldehyde, 1% sodium metabisulfite (SMB) containing 0.1 M cacodylate, pH 7.2, and incubated for 1 hour at room temperature (Sinakevitch et al., 2001). Following fixation, cells were washed twice with Tris-SMB (0.5% SMB, 0.05 M Tris-HCl, pH 7.5) and incubated for 10 minutes in 0.1 M sodium borohydride in Tris-SMB. After three washes in Tris-SMB, cells were incubated overnight with 10% fetal bovine serum (FBS) in Tris-SMB with 0.5% Triton X-100. Next, cells were incubated with rabbit anti-glutamate antibody diluted 1/500 in block buffer [2% bovine serum albumin (BSA), 1% fish-skin gelatin, 0.02% saponin in PBS, pH 7.4] for 2 hours at room temperature. The cells were washed three times for 5 minutes each with the same buffer and incubated with Alexa-488-conjugated goat anti-rabbit antibody diluted 1/1000. Cells were washed as described and maintained in ice-cold PBS until processed. Non-specific staining was determined by incubating anti-glutamate antibodies with a BSA-glutaraldehyde-glutamate conjugate (BGG) (Geffard et al., 1984). To assess vesicular pools of glutamate, cells were incubated in the absence or presence of 200 nM bafilomycin A1.

Vesicular index

Vesicular index was calculated as [(FC–BGG)–(FB–BGG)÷(FC–BGG)] where FC is the mean fluorescence in the absence of bafilomycin A1, FB is the mean fluorescence in the presence of bafilomycin A1 and BGG is the mean fluorescence in the presence of BGG. Thus, if there was no vesicular glutamate, the vesicular index should be 0, because FC=FB.

Results

Vglut1 is present in ZnT3-containing vesicles

In order to analyse whether ZnT3 transport activity could be under control of the glutamate transporter Vglut1, we first determined whether ZnT3 and Vglut1 were segregated to the same vesicle population. Clonal PC12 cells doubly transfected with Vglut1 and ZnT3 (VglZn cells) were treated with or without brefeldin A (BFA) for 2 hours at 37°C (Fig. 1). This drug interferes with ARF-dependent vesicle-formation mechanisms and blocks the biogenesis of endosome-derived AP-3-dependent microvesicles while sparing the ARF1-independent plasma-membrane route of SLMV biogenesis in PC12 cells (Faundez et al., 1997; Salazar et al., 2004a; Salazar et al., 2004b). Cells were homogenized and high-speed (S2) supernatants were fractionated on glycerol velocity gradients. SLMV fractions peaked in the middle of the gradient. The BFA-sensitive fractions were detected using antibodies against ZnT3 (Fig. 1A) (Salazar et al., 2004a; Salazar et al., 2004b), whereas BFA-insensitive vesicles were monitored with the synaptic-vesicle antigen synaptophysin (Fig. 1A) (Salazar et al., 2004a; Salazar et al., 2004b). After BFA treatment, SLMV Vglut1 content decreased to half of the control values (n=2), indicating that a significant proportion of Vglut1 co-segregates with ZnT3. The BFA effect upon Vglut1 targeting to SLMV is independent of the ZnT3 content (Fig. 1B). After BFA treatment, Vglut1 decreased similarly in vesicles isolated from

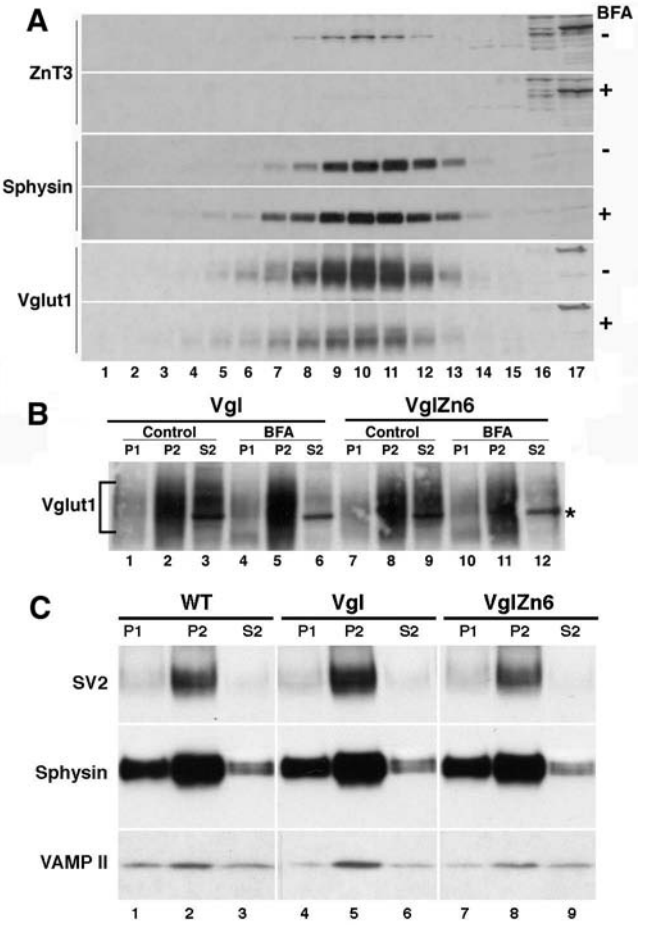

Fig. 1. Vglut1 and ZnT3 targeting to SLMVs are sensitive to brefeldin A. (A) PC12 cells transfected with Vglut1 and ZnT3 (VglZn clone 6 cells, VglZn6) were incubated in the absence or presence of 10 μg ml^{-1} BFA for 2 hours at 37°C. Cells were homogenized and equal protein amounts of S2 supernatant were resolved by glycerol-gradient sedimentation. Gradient fractions were analysed by immunoblot with antibodies against ZnT3, Vglut1 and synaptophysin (Sphysin). BFA decreased Vglut1 and ZnT3 targeting to SLMVs without affecting synaptophysin levels. (B) PC12 cells either expressing Vglut1 (Vgl cells) or co-expressing Vglut1 and ZnT3 (VglZn cells) were incubated in the absence or presence of BFA. Cell homogenates were fractionated and membrane fractions (P1, P2 and S2) were analysed by immunoblot with Vglut1 antibodies. After BFA treatment, Vglut1 decreases from the SLMV-enriched fraction (S2) independent of ZnT3 expression. The bracket on the left marks the migration of Vglut1, which characteristically migrates as a broad band (see Fig. 6B) (Bellocchio et al., 1998; Takamori et al., 2000a; Takamori et al., 2000b). Asterisk represents a cytosolic background band. (C) Untransfected cells (wt), PC12 clones expressing Vglut1 (Vgl) or Vglut1 and ZnT3 (VglZn) were fractionated by differential centrifugation and S2 enriched SLMV fractions were analysed by immunoblot using antibodies against the synaptic-vesicle markers SV2, synaptophysin (Sphysin) and VAMP II. Overexpression of transporters does not modify the SLMV content (n=3).

PC12 cells expressing either Vglut1 only (Fig. 1B, Vgl, compare lane 3 and 6) or cells expressing exogenous ZnT3 and Vglut1 transporters (Fig. 1B, VglZn, compare lanes 9 and 12), thus indicating that Vglut1 targeting to SLMV is not modified

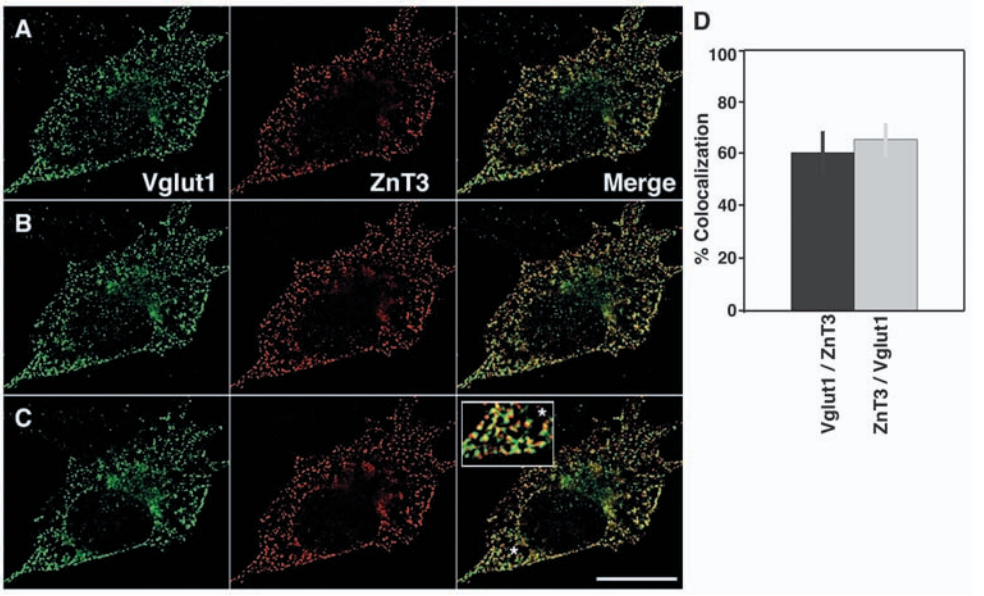

Fig. 2. Vglut1 and ZnT3 colocalize in PC12 cells. PC12 cells expressing ZnT3 and Vglut1 were double labeled with antibodies against the HA tag present in ZnT3 and antibodies against Vglut1. Cell were imaged by wide-field deconvolution microscopy and colocalization was determined by Metamorph software using ten randomly picked cells. (A-C) Optical sections from the bottom of the cell to the top, spaced every 0.75 μm.

by the expression of ZnT3. Moreover, expression of these transporters did not modify the overall subcellular distribution or content of synaptic-vesicle markers (Fig. 1C) in SLMV fractions. The amount of SV2, synaptophysin and VAMP II were indistinguishable among S2 fractions enriched in SLMVs isolated from either untransfected or transfected cells (Fig. 1C, lanes 3,6,9).

The effects of BFA on ZnT3 and Vglut1 suggested that these transporters were targeted to the same organelles. To test this hypothesis, we performed immunolocalization and vesicle-adsorption assays using antibodies against Vglut1 and the tag engineered in ZnT3. Wide-field deconvolution microscopy revealed that ZnT3- and Vglut1-positive organelles extensively colocalized (Fig. 2A-C). Metamorph analysis indicated that 60.8±8.0% of Vglut1-positive puncta colocalized with ZnT3 (Fig. 2D, n=10). Similarly, 65.5±5.5% of ZnT3-positive organelles colocalized with Vglut1 (Fig. 2D). To confirm that ZnT3 and Vglut1 transporters coexisted on the same organelles, we performed immunomagnetic isolations of glycerol-enriched SLMV fractions from VglZn cells. Beads were coated with monoclonal antibodies against a cytosolic epitope present in Vglut1 and captured vesicles were monitored by immunoblot with polyclonal antibodies against ZnT3 and Vglut1. Control immunoadsorptions with antibodies against the lumenal domain of LAMP I bound neither Vglut1- or ZnT3-positive membranes (Fig. 3A, lane 1), and most of the vesicle antigens remained in the unbound fraction (Fig. 3B, lane 1). Under this conditions 83.3±21.4% (n=9 in three experiments, average±s.d.) of the ZnT3 input was recovered in beads coated with Vglut1 antibodies demonstrating that Vglut1 and ZnT3 were present in a common vesicle population.

The effects of BFA on transporter targeting in PC12 cells prompted us to examine whether Vglut1 was targeted by AP-3-dependent mechanisms. In PC12 cells, endosome-derived microvesicles carrying synaptic-vesicle markers retain in part their AP-3 adaptor coat (G. Salazar, B. Craige and V. Faundez, unpublished). Similarly, SLMV fractions isolated with anti-Vglut1 antibodies contained AP-3 complexes detected with anti-β3 antibodies (Fig. 3C, lanes 2,3). This interaction was specific because no AP-3-immunoreactive bands were detected in control anti-LAMP-antibody-coated beads (Fig. 3C, lane 1). Furthermore, immunomagnetic isolation of SLMV fractions with antibodies against AP-3 δ captured Vglut1-containing

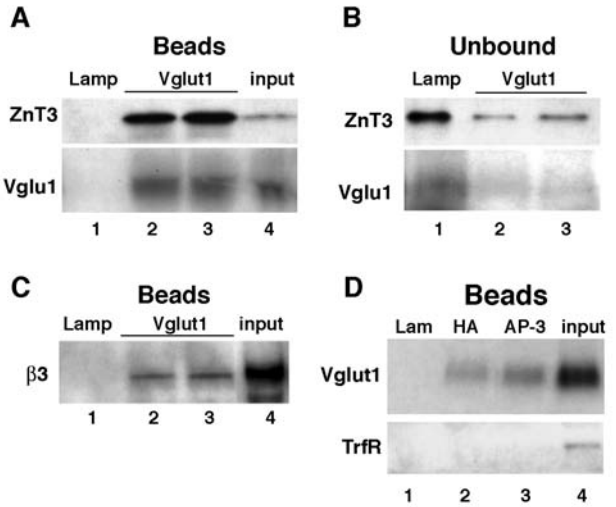

Fig. 3. Vglut1 and ZnT3 are targeted to a common vesicle population. A glycerol gradient isolated SLMV fractions derived from Vglut1 and ZnT3HA (VglZn) double-transfected PC12 cells, and these were immunomagnetically isolated with beads coated with monoclonal antibodies against Vglut1 (A-C), antibodies against the HA tag present in ZnT3 (D, lane 2) or a monoclonal antibody against the AP-3 δ subunit (D, lane 3). Control assays were performed with beads coated with an antibody against a lumenal epitope of LAMP I. Bead-bound vesicles were resolved by SDS-PAGE and analysed by immunoblot with polyclonal antibodies against Vglut1, ZnT3 and the AP-3 β3 subunit, and a monoclonal anti-transferrin-receptor (TrfR) antibody. (B) Unbound membranes were sedimented at high speed and analysed in parallel with bead-bound organelles depicted in (A,D). The Vglut1 blot was exposed for 30 seconds, whereas the TrfR blot was exposed overnight. Inputs correspond to 10%. Lanes 2 and 3 (A-C) represent duplicate assays.

membranes (Fig. 3D, lane 3). This interaction was selective because, in addition to the LAMP control (Fig. 3D, lane 1), Vglut1-positive vesicles were devoid of contaminant endosomes detected with anti-transferrin-receptor antibodies (Fig. 3D, lane 3).

We further explored whether Vglut1 was targeted by AP-3-dependent mechanisms by analysing the targeting of this transporter to synaptic vesicles isolated from AP-3-deficient mouse brains (Salazar et al., 2004a; Salazar et al., 2004b). We have established that synaptic-vesicle proteins whose targeting to synaptic vesicles is sensitive to AP-3 either selectively decrease their content in synaptic-vesicle fractions and/or appear in faster-migrating membranes in AP-3-deficient brain (Salazar et al., 2004a; Salazar et al., 2004b; Seong et al., 2005). These phenotypes are more pronounced in mocha neurons lacking both ubiquitous and neuronal AP-3 isoforms (Kantheti et al., 1998) than in neurons selectively deficient in neuronal AP-3 complexes (*Ap3b2*$^{-/-}$) (Seong et al., 2005). As previously reported (Salazar et al., 2004a; Salazar et al., 2004b), synaptophysin vesicle content and sedimentation were indistinguishable between wild-type and AP-3-deficient brain vesicles (Fig. 4A), yet ZnT3 was severely reduced in mocha brain (Fig. 4A) (Salazar et al., 2004a; Salazar et al., 2004b). Vglut1-containing mocha vesicles consistently and significantly sedimented faster than wild-type membranes by one fraction (Fig. 4A,B; n=3). Moreover, in the absence of AP-3, one-quarter of the Vglut1 transporter did not reach brain synaptic vesicles (Fig. 4C, n=3, P=0.032). These phenotypes are similar to, although milder than, those described for chloride channel 3 in mocha brain (Salazar et al., 2004a; Salazar et al., 2004b). The subtle Vglut1 phenotype detected in mocha brain synaptic vesicles was not appreciable in synaptic vesicles from the neuronal AP-3-deficient mouse brain (Fig. 4D, *Ap3b2*$^{-/-}$), consistent with our observation of a decreased phenotype penetrance in this genetic background (Seong et al., 2005). In summary, genetic, biochemical and pharmacological evidence indicates that some Vglut1 is targeted to vesicles by AP-3-dependent mechanisms.

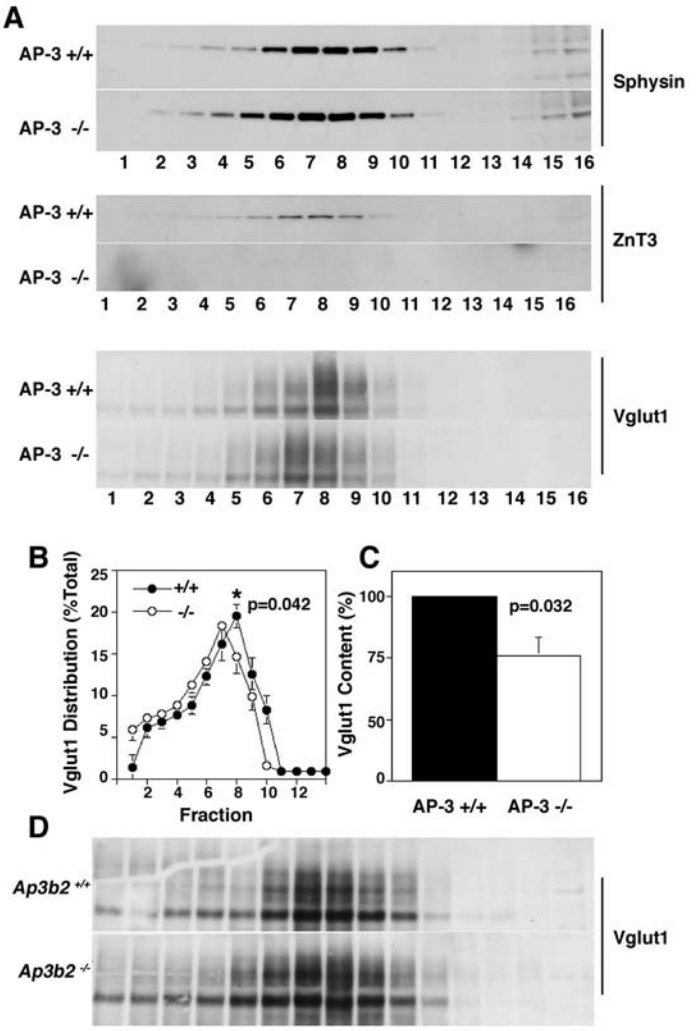

Fig. 4. Vglut1 and ZnT3 targeting to AP-3-deficient brain synaptic vesicles. (A) High-speed supernatants (S2) from wild-type (+/+) and mocha (–/–) brain homogenates were fractionated in 5-25% glycerol gradients to resolve small vesicles. Synaptic-vesicle antigen levels across gradients were determined by immunoblot using antibodies against synaptophysin (Sphysin), ZnT3 and Vglut1. ZnT3 and Vglut1 sedimentation patterns and the antigen contents of the membranes were altered in mocha brain vesicles. (B) The normalized content distribution of Vglut1 (n=3). No differences were found in the normalized distribution of synaptophysin (Kantheti et al., 1998; Salazar et al., 2004a). Closed circles represent wild-type membranes, open circles mocha vesicles. (C) The Vglu1 synaptic-vesicle level was determined in the peak fractions. The content of Vglut1 (n=3) was selectively reduced in mocha compared with control brain membranes. No changes were detected in the synaptophysin synaptic-vesicle levels (Kantheti et al., 1998; Salazar et al., 2004a). (D) S2 supernatants were obtained from wild-type (*Ap3b2*$^{+/+}$) and neuronal AP-3-deficient brains (*Ap3b2*$^{-/-}$) and fractionated as described in A. No appreciable differences were observed between brains lacking neuronal AP-3 and brains lacking both neuronal and ubiquitous AP-3 (n=3). ZnT3 synaptic-vesicle levels were partially affected in *Ap3b2*$^{-/-}$ (Seong et al., 2005).

Co-targeting of glutamate and zinc transporters increases vesicular zinc incorporation

Once we had determined that Vglut1 and ZnT3 coexist in overlapping vesicle populations, we analysed whether zinc transport mechanisms into the vesicle lumen could be modulated by the presence of Vglut1. Zinc content was analysed using the zinc-selective fluoroprobe zinquin (Fig. 5) (Nasir et al., 1999; Zalewski et al., 1993). We explored whether zinquin staining was vesicular and colocalized with synaptic-vesicle markers in PC12 cells. In vivo two-photon microscopy of NGF-differentiated PC12 cells demonstrated that zinquin was contained in discrete vesicles. Importantly, these vesicles did not localize with syntaxin-13/GFP, a marker of the early endosomes (Prekeris et al., 1998), which give rise in PC12 cells to BFA-sensitive AP-3 microvesicles (de Wit et al., 1999; Lichtenstein et al., 1998). However, zinquin fluorescence localized well with that of the synaptic-vesicle marker GFP/VAMP-II in both undifferentiated PC12 cells (not shown) and the cell bodies and processes of NGF-differentiated PC12 cells (Fig. 5C).

Vesicular zinquin fluorescence was analysed by quantitative flow cytometry. In wild-type PC12 cells (WT), the zinquin signal was nine times higher than in unstained cells (NS) (Fig. 6A) and a small proportion of this fluorescence was sensitive

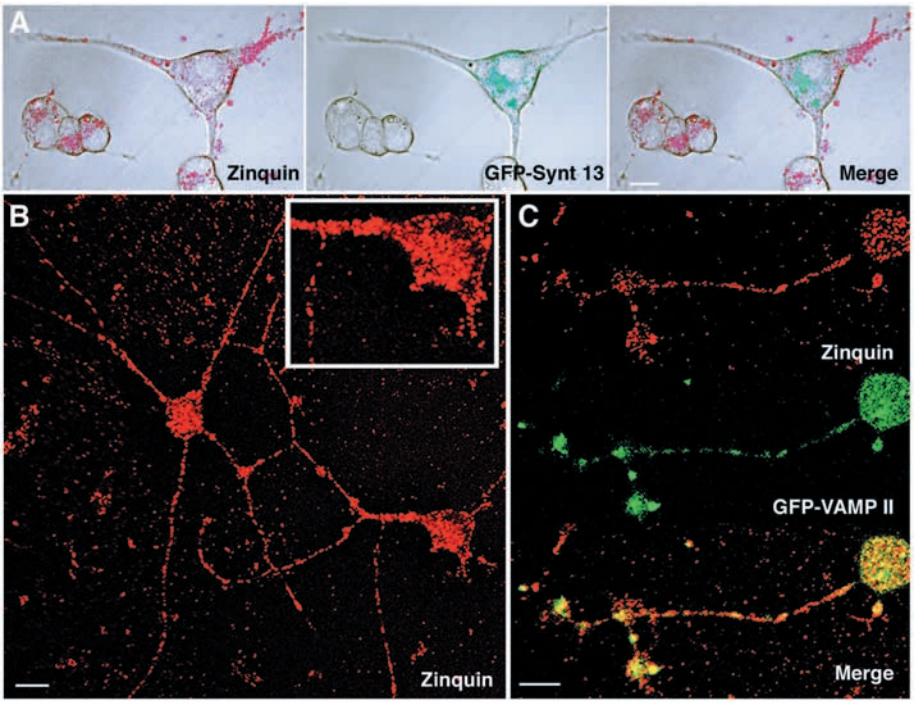

Fig. 5. Zinquin colocalizes with the synaptic-vesicle marker VAMP II in differentiated PC12 cells. (A) NGF-differentiated PC12 cells transfected with the early endosome marker syntaxin-13/GFP were zinc loaded, stained with zinquin and imaged by two-photon microscopy. Zinquin puncta and syntaxin-13/GFP failed to colocalize. (B) NGF-differentiated PC12 cells accumulate zinquin in vesicular compartments that (C) co-localize with the synaptic-vesicle marker VAMP-II/GFP.

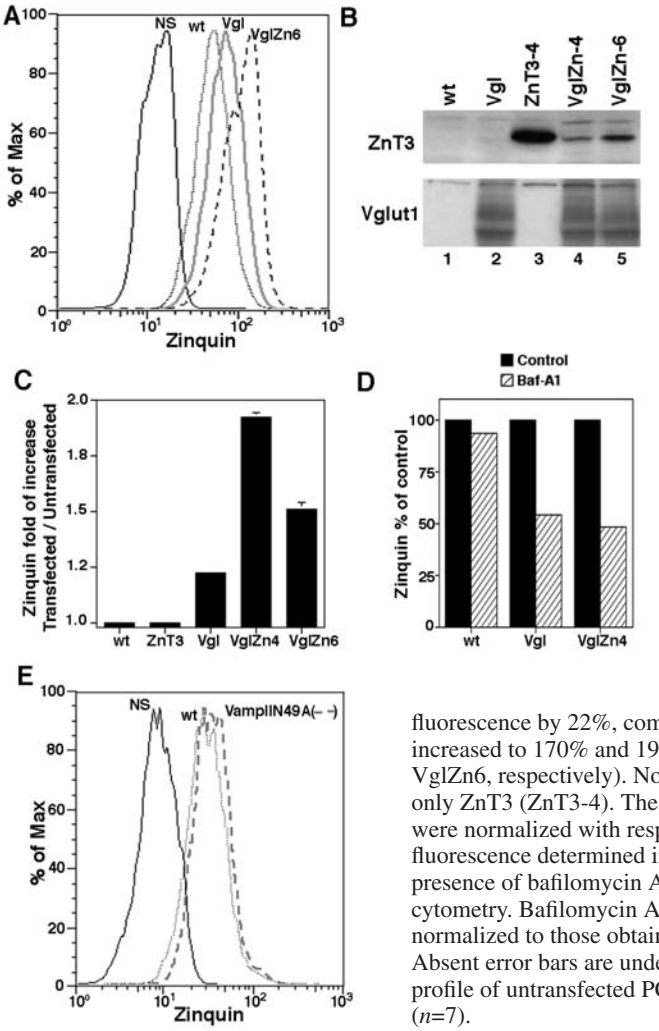

to bafilomycin A1 (Fig. 6D), a drug that selectively inhibits the vacuolar ATPase (vATPase) and effectively depletes synaptic vesicles of neurotransmitters (Zhou et al., 2000). PC12 cells express low endogenous levels of ZnT3 (Fig. 6B) (Salazar et al., 2004b), but increasing ZnT3 production levels in SLMV fractions did not affect zinc incorporation as determined by zinquin fluorescence (Fig. 6C, 100.7±1.8%, n=10) (Salazar et al., 2004a; Salazar et al., 2004b), indicating that ZnT3 itself is not the rate-limiting step in vesicular zinc uptake. These results are consistent with those reported by Palmiter et al. for non-neuronal BHK cells (Palmiter et al., 1996). However, in PC12 cells producing Vglut1 (Vgl cells), the low endogenous ZnT3 levels were enough to support a 22.0±5.2% (n=11) increase in vesicular zinc content and to make almost half of the cells' total zinc uptake bafilomycin-A1 sensitive (Fig. 6A,C,D). Co-expression of both ZnT3 and Vglut1 transporters further

Fig. 6. Vglut1 increases the steady-state vesicular zinc content. Untransfected PC12 cells (wt), clones carrying either Vglut1 (Vgl), Vglut1 and ZnT3 (VglZn) or the VAMP II N49A mutant were zinc loaded and stained with zinquin. Zinquin fluorescence was determined by flow cytometry (A,C-E). (B) Immunoblot analysis of the expression levels of ZnT3 and Vglut1 in the cell types used in A,C-D. (A-C) Expression of Vglut1 (Vgl) increased zinquin fluorescence by 22%, comparing wild-type (wt) and Vgl cells. Zinquin fluorescence was further increased to 170% and 196% in two different clones co-expressing Vglut1 and ZnT3 (VglZn4 and VglZn6, respectively). No difference in zinquin fluorescence was observed in a PC12 clone carrying only ZnT3 (ZnT3-4). The graph depicts the average mean values of flow-cytometry profiles. Data were normalized with respect to untransfected PC12 cells (100%). 'NS' is the background fluorescence determined in unstained cells. (D) Zinc loading was carried out in the absence or presence of bafilomycin A1 and zinc content was determined by zinquin fluorescence and flow cytometry. Bafilomycin A1 decreases zinquin fluorescence in Vgl and VglZn clones. Values are normalized to those obtained in the absence of drug (100%) for each cell type. Average ± s.e.m. Absent error bars are under the graphing threshold. (E) Representative zinquin flow-cytometry profile of untransfected PC12 cells (wt) and a PC12 clone carrying the VAMP II N49A mutant (n=7).

increased the zinc accumulation by 70.0±11% (n=9) and 92.0±2.9% (n=4) in two independent clones compared with PC12 cells carrying either endogenous or exogenously expressed ZnT3 (Fig. 6A,C). Four other different clones showed similar increments. Notably, the VglZn clones expressed less ZnT3 (Fig. 6B) than the ZnT3-4 clonal cell line, yet Vgl and VglZn cells carried similar levels of Vglut1 (Fig. 6B). The vesicular nature of the increased zinquin fluorescence was assessed with bafilomycin A1 (Fig. 6D). This drug decreased the zinquin signal to 54.5±0.35% and 48.0±0.07% of the value observed in Vgl and VglZn-4 cell lines (n=2), respectively. These results suggest that, in the absence of Vglut1, ZnT3-dependent transport needs ancillary mechanisms to accumulate zinc efficiently into vesicles. To determine whether the effects of increased expression of transporters upon zinquin fluorescence were specific, we tested a cell line overexpressing the VAMP II N49A mutant. This mutant protein is preferentially targeted to SLMV fractions by BFA-sensitive mechanisms (Faundez et al., 1997; Shi et al., 1998). Cells overexpressing the VAMP II N49A mutant did not modify their zinquin fluorescence (Fig. 6E), indicating that increased zinquin staining is not a generalized response to augmented membrane-protein expression in SLMV fractions. In summary, these results show that ZnT3 expression is not sufficient to increase vesicular zinc uptake and that the vesicular glutamate transporter Vglut1 is required for effective vesicular zinc transport. Moreover, our findings provide functional evidence supporting the hypothesis that a pool of Vglut1 and ZnT3 are co-targeted to the same vesicle population.

Co-targeting of glutamate and zinc transporters stimulates vesicular glutamate uptake

If Vglut1 transport activity mediates the increased vesicular zinc uptake then vesicular levels of glutamate should increase in cells carrying both ZnT3 and Vglut1. We measured uptake of radiolabeled glutamate into cytosol-free isolated SLMV fractions (Bellocchio et al., 2000). Expression of Vglut1 conferred valinomycin-sensitive glutamate uptake on vesicles isolated from PC12 cells expressing Vglut1 (Fig. 7A). By contrast, glutamate uptake was similar in the absence or presence of the drug in untransfected PC12 cells (Fig. 7A), indicating that SLMV membranes lack glutamate transport activity. We next compared glutamate uptake into vesicles isolated from Vgl or VglZn cells in the absence or presence of $ZnSO_4$. As previously described, supplementation of ionic zinc above the cytoplasmic free-zinc concentration inhibited glutamate transport in a dose-dependent manner (Naito and Ueda, 1985). However, vesicles containing both Vglut1 and ZnT3 (VglZn) increased their glutamate uptake 1.42±0.7 times (n=8, P<0.001) at low nanomolar concentrations of ionic zinc. To explore further in intact cells whether zinc stimulated vesicular glutamate uptake, we developed a novel intact-cell assay comparable to our zinquin flow cytometry. Our method relies on a flow-cytometry-based glutamate-immunodetection procedure using anti-glutamate antibodies to determine steady-state levels of vesicular glutamate. The specificity of glutamate antibodies has been extensively characterized (Somogyi et al., 1986; Storm-Mathisen et al., 1983; Storm-Mathisen et al., 1986). Moreover, these antibodies are a standard tool for identifying glutamatergic neurons in nerve tissue (Bramham et al., 1990; Somogyi et al., 1986). Glutamate antibodies recognize glutamate conjugated to glutaraldehyde generated during fixation. This immunoreactivity can be abolished using the BGG conjugate as a competitor. We first confirmed the vesicular nature of glutamate by immunofluorescence of PC12 cells transfected with Vglut1 (Vgl, Fig. 8A). A prominent signal localized to cytoplasmic vesicles. Moreover, the vesicular immunostaining was abolished in the presence of BGG conjugate, confirming the specificity of the antibody (Fig. 8A, right).

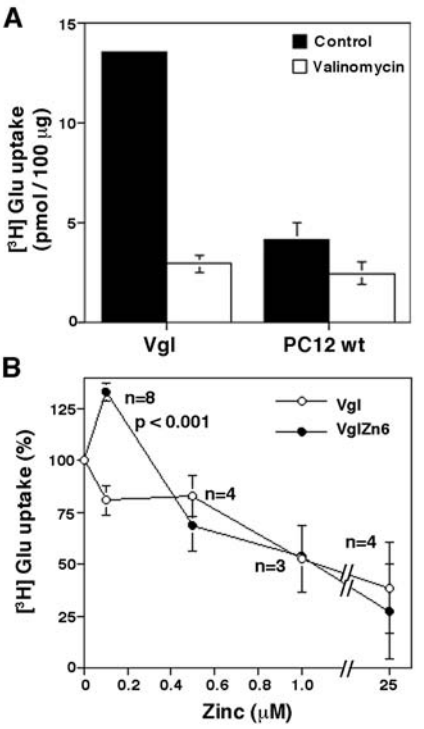

Fig. 7. Zinc increases in vitro vesicular glutamate uptake. (A) SLMV-enriched fractions were prepared from untransfected (wt) and Vglut1-transfected (Vgl) cells. Vesicle-specific [^{3}H]-glutamate uptake was determined in either the absence or the presence of the ionophore valinomycin (20 μM). Vesicular glutamate uptake is detected only in SLMV fractions from Vglut1-transfected cells (n=2). (B) [^{3}H]-Glutamate uptake was performed in either the absence or the presence of increasing concentrations of ionic zinc ($ZnSO_4$). Equal amounts of Vgl and VglZn6 SLMV protein were used in all assays. The protein content per assay was confirmed by immunoblot using antibodies against synaptic-vesicle markers.

Glutamate immunoreactivity was measured by flow cytometry in untransfected cells and in clonal cells carrying either only Vglut1 (Vgl) or both Vglut1 and ZnT3 (VglZn). Expression of Vglut1 alone increased the glutamate content in PC12 cells by 56.0±6.9% (Fig. 8B,D; P<0.001, n=6) compared with untransfected cells. Importantly, Vglut1 expression conferred bafilomycin-A1-sensitive glutamate uptake on PC12 cells confirming its vesicular nature (Fig. 8E). These results recapitulate vesicular glutamate uptake previously shown in isolated membrane fractions in the same cells (Bellocchio et al., 2000). Co-expression of both Vglut1 and ZnT3 transporters further increased the glutamate immunoreactivity to

88.3±5.3% (Fig. 8B,D, VglZn4 clone, n=11, P<0.001). We observed a similar increment in several other independent clones (Fig. 8B,D, VglZn6 clone, 80.0±3.8%, n=10, P<0.001). To exclude the possibility that these differences in glutamate uptake between Vgl and VglZn cells could be due to higher Vglut1 expression in VglZn cells, we determined their Vglut1 content by immunoblot (Fig. 6B) and flow cytometry using Vglut1 antibodies (Fig. 8C) both in Vgl and VglZn cells. Vglut1 expression was slightly lower in VglZn clonal cells than the parental Vgl cells (89.4±2.0% VglZn4 and 86.6±0.45% VglZn6 cells, n=4), thus ruling out the possibility that the higher vesicular glutamate immunoreactivity observed in ZnT3/Vglut1-expressing cells was caused by increased Vglut1 levels.

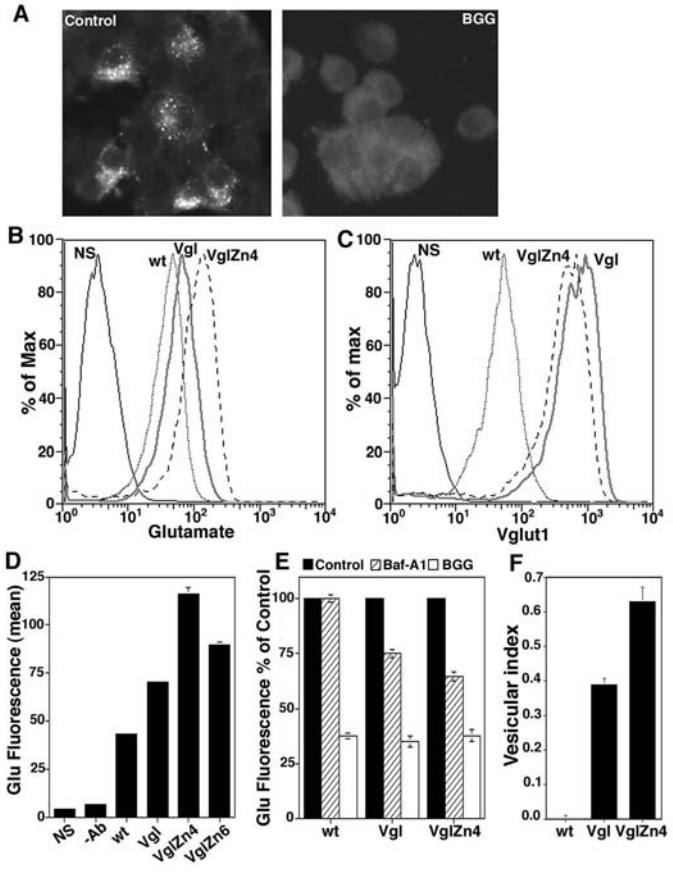

Fig. 8. Co-expression of zinc and glutamate transporters increases the steady-state vesicular glutamate content in whole cells. Untransfected PC12 cells (wt) or transfected either with Vglut1 (Vgl) or co-transfected with Vglut1 and ZnT3 (VglZn) were stained with glutamate (A,B,D,E) or Vglut1 antibodies (C). (A) Glutamate staining was mainly vesicular and was abolished by the BGG. Glutamate cellular content (B,D) increased in the presence of Vglut1 (Vgl) and co-expression of ZnT3 and Vglut1 further increased the cellular levels of glutamate (VglZn clones 4 and 6). NS, unstained cells; –Ab, cells stained only with the secondary antibody. (C) VglZn4 clonal cells produce less Vglut1 transporter than Vgl cells. (E) PC12 cells or clonal variants were treated in the absence or presence of bafilomycin A1 before antibody staining. Values are normalized to those obtained in the absence of drug (100%) for each cell type. (F) The vesicular index, representing vesicular glutamate pools, was 1.6 times greater in VglZn than in Vgl cells. Average ± s.e.m. Absent error bars are under the graphing threshold.

Glutamate immunoreactivity in Vgl and VglZn cells is mainly vesicular (Fig. 8A). However, non-vesicular glutamate pools present in these cells could contribute to the total glutamate immunoreactivity determined by flow cytometry. In order to analyse the contribution of Vglut1 and ZnT3 to the vesicular glutamate uptake, we defined a vesicular index by measuring the pool of glutamate immunoreactivity sensitive to bafilomycin A1. PC12 cells lack detectable Vglut1 transporter protein either by immunoblot (Fig. 6C, lane 1) or functional glutamate uptake assays (Fig. 7A), so the endogenous glutamate pool should be predominantly non-vesicular. In fact, the bafilomycin-sensitive pool of glutamate immunoreactivity was negligible in these cells, and the vesicular index was almost 0 (Fig. 8F). By contrast, cells expressing Vglut1 (vesicular index 0.39±0.035) or both transporters (vesicular index 0.64±0.07) acquired a bafilomycin-sensitive glutamate pool, yet this pool was consistently larger in ZnT3/Vglut1- than in Vglut1-expressing cells (Fig. 8E). Thus, the presence of ZnT3 increases the vesicular glutamate pools 1.6 times. These observations are in agreement with our in vitro glutamate uptake assays (Fig. 7B) and collectively support the hypothesis that the transport activity of Vglut1 regulates vesicular zinc uptake. In conclusion, our results show that Vglut1 and ZnT3 are targeted to an overlapping vesicle population by AP-3-dependent mechanisms. In this common vesicle population, the transporters mutually regulate the incorporation of zinc and glutamate into vesicles.

Discussion

Small-molecule transport into synaptic vesicles has been analysed mainly in the context of individual neurotransmitter transport mechanisms (Reimer et al., 2001). These processes are driven by the proton gradient generated by the activity of the vacuolar ATPase (Reimer et al., 2001). However, whether synaptic-vesicle individual-neurotransmitter transport mechanisms reciprocally influence the activity of other transporters present on the same vesicles has not been analysed. To explore how different transporters present on the same vesicle might functionally interact, we first addressed the question of whether a common targeting mechanism delivers different transporters into the same vesicle population. We then asked whether distinct yet co-targeted transport mechanisms jointly regulate vesicle lumenal composition. We focused on the zinc transporter ZnT3 and the vesicular glutamate transporter Vglut1, two transporters present in synaptic vesicles and prominently expressed in brain nerve terminals that release both zinc and glutamate (Bellocchio et al., 1998; Huang, 1997; Takeda, 2000; Wenzel et al., 1997). We used neuroendocrine PC12 cells because, in these cells, the adaptor-dependent mechanisms controlling the targeting of synaptic vesicle proteins can be biochemically and pharmacologically studied, and because different neurotransmitter transport mechanisms have been successfully reconstituted by gene transfection. We show that about half of the Vglut1-positive vesicles also contain ZnT3, using complementary pharmacological, microscopy and biochemical tools. In PC12 cells, AP-2 and AP-3 targeting mechanisms to SLMV fractions can be selectively inhibited by plasma-membrane cholesterol depletion or BFA treatment, respectively (Salazar et al., 2004b). In the present study, we have determined that half of

the Vglut1 targeting to SLMV fractions is sensitive to BFA (Fig. 1A), whereas 40% is sensitive to inhibitors of the plasma-membrane-derived SLMV biogenesis (Salazar et al., 2004b). Consistent with these observations, one-quarter of the Vglut1-transporter pool in brain is targeted to synaptic vesicles using the adaptor complex AP-3 (Fig. 4B). Moreover, we have been able biochemically to document the Vglut1 transporter present in AP-3-coated intermediaries isolated from PC12 cells (Fig. 3C,D). Thus, Vglut1 uses complementary AP-2- and AP-3-based machineries to reach SLMV fractions, sharing the AP-3 pathway with ZnT3.

Exogenous expression of neurotransmitter transporters in PC12 cell vesicles recapitulates their functional properties found in brain vesicles (Bellocchio et al., 2000; Liu and Edwards, 1997; Schafer et al., 2002; Varoqui et al., 2002). PC12 cells offer a homogeneous neuronal-like cellular system lacking Vglut1 and capable of controlled ZnT3 and Vglut1 expression. PC12 cells lack detectable Vglut1 protein (Fig. 6B) but, more importantly, isolated SLMV do not possess in vitro glutamate transport activity (Fig. 7A), excluding the presence of other vesicular glutamate transporters in these membranes. Our data show that ZnT3 and Vglut1 co-targeting to the same vesicle population jointly regulates zinc and glutamate uptake into vesicles. The increased transport activities are neither a consequence of an enlarged SLMV pool after transporter overexpression (Fig. 1C) nor the outcome of increased membrane protein levels in SLMV fractions (Fig. 6E). In vitro, zinc stimulates uptake of glutamate at low concentrations yet, as previously described, this metal is inhibitory at micromolar concentrations (Naito and Ueda, 1985) (Fig. 7B). The significance of the zinc-induced increase in glutamate uptake in vitro relies on the observation that the effects of zinc are only apparent in vesicles isolated from cells simultaneously expressing ZnT3 and Vglut1 (Fig. 7B) but not from those expressing only Vglut1. The inhibitory effects of zinc upon glutamate uptake at higher concentrations might derive from the mechanism by which zinc is presented to transporters in vivo. In intact cells, cytosolic zinc rather than being present as free ions remains bound to metallochaperones such as metallothioneins (Aschner et al., 1997). Therefore, it was important to test glutamate uptake mechanisms in intact P12 cells incubated in physiological concentrations of extracellular zinc.

Using an antibody-based immunodetection procedure, we have demonstrated that expression of Vglut1 in PC12 cells confers, at the steady state, bafilomycin-A1-sensitive accumulation of glutamate in vesicular compartments. The use of flow cytometry and the definition of the vesicular index provide quantitative estimates in neurotransmitter content allowing us to explore the functional consequences of ZnT3 expression upon vesicular glutamate uptake. Our in vivo glutamate uptake assays are in good agreement with the in vitro transport determinations. First, in the absence of Vglut1, there is no detectable vesicular pool of glutamate in vivo, a pool defined by its bafilomycin-A1 sensitivity. Similarly, in the absence of Vglut1 expression, there is no detectable valinomycin-sensitive uptake of [^{3}H]-glutamate into vesicles in vitro. Second, in whole cells, the combined expression of ZnT3 and Vglut1 increases the glutamate vesicular pool 1.6 times compared with cells expressing Vglut1 only; this value is in harmony with the 1.42-times increase observed with isolated membranes. Likewise, we developed an intact-cell assay to assess vesicular zinc under conditions in which the transport of glutamate into vesicles was modified. This procedure is based on quantitative flow cytometry of the zinc-specific fluorescent probe zinquin (Nasir et al., 1999; Zalewski et al., 1993). Zinc pools revealed by zinquin are vesicular as determined by two-photon microscopy (Fig. 5) and bafilomycin-A1 sensitivity (Fig. 6C,D). Endogenous levels of ZnT3 in PC12 cells are low and incapable of conferring bafilomycin-A1-sensitive vesicular zinc uptake. Furthermore, overproduction of ZnT3 does not initiate bafilomycin-A1-sensitive vesicular zinc transport, indicating that ZnT3 requires ancillary mechanisms for efficient vesicular zinc storage. Glutamate transport fulfills this ancillary role. The low endogenous ZnT3 levels are enough to render zinc uptake bafilomycin-A1-sensitive by expression of Vglut1. These results indicate that the rate-limiting factor in zinc transport is not the availability of ZnT3 but rather the Vglut1 transport activity. Although other unidentified zinc transporters present in PC12 cells could play a role in the mechanism already described, we believe that ZnT3 plays a major role. ZnT3 targeting to synaptic vesicles is specific because ZnT4 produced at high levels in PC12 cells is excluded from synaptic vesicles (data not shown). If other transporters were to be involved, they should be targeted to synaptic vesicles, yet the *ZnT3*$^{-/-}$ mice suggest otherwise because of their lack of synaptic-vesicle ionic zinc (Cole et al., 1999). Collectively, our results indicate that ZnT3 and Vglut1 mutually regulate each other's transport activities and modify the lumenal composition of secretory vesicles.

Bacterial and synaptic vesicle members of the zinc-transporter family transport metal by a proton-coupled-antiporter mechanism (Chao and Fu, 2004; Colvin et al., 2000a; Colvin et al., 2000b). In bacteria, the antiporter mechanism occurs with a stoichiometry of metal ion to proton close to 1:1 (Chao and Fu, 2004). In synaptic vesicles, lumenal zinc accumulation is associated with vesicle alkalinization (Colvin et al., 2000a; Colvin et al., 2000b). Zinc accumulation probably increases the electrical gradient across the synaptic vesicle membrane while increasing the intravesicular pH, thus making the vesicle lumen more positive and favoring vesicular glutamate uptake (Reimer et al., 2001). Glutamate could be driven into the vesicle lumen as part of an anionic shunt. This explanation is consistent with our results that increased expression levels of a synaptic-vesicle chloride channel are associated with increased vesicular zinc stores (Salazar et al., 2004a). Ablation of intravesicular zinc, like in *ZnT3*$^{-/-}$ mouse, would decrease the transvesicular electrical gradient thereby reducing the vesicular glutamate content. Consequently, a coordinated reduction in a vesicular inhibitory neuromodulator, zinc, and the excitatory agonist, glutamate, could have negligible effects on the postsynaptic N-methyl-D-aspartate (NMDA) receptor responses. Our results suggest that coupling ZnT3 and Vglut1 transport activities insures that individual synaptic vesicles contain appropriate concentrations of excitatory and inhibitory neurotransmitter and neuromodulators. The functional coupling between the zinc and glutamate vesicular transport mechanisms could explain the apparent contradiction of a normal NMDA-dependent neurotransmission in *ZnT3*$^{-/-}$ mouse models (Lopantsev et al., 2003) and the powerful negative effects that zinc exerts upon

NMDA receptors as revealed by chelation of synaptic released zinc (Ueno et al., 2002; Vogt et al., 2000). Coupled storage into synaptic vesicles of both zinc and excitatory neurotransmitters could regulate the postsynaptic functional consequences of released vesicular glutamate. We propose that this functional transport coupling provides a vesicular mechanism to control glutamate-mediated toxicity.

Supported by NIH RO1 NS42599 and CAM Pilot Project Grant. We appreciate the comments of L. Li, C. Hartzell, B. Wainer, E. Werner and A. P. Kowalczyk.

References

Aschner, M., Cherian, M. G., Klaassen, C. D., Palmiter, R. D., Erickson, J. C. and Bush, A. I. (1997). Metallothioneins in brain – the role in physiology and pathology. *Toxicol. Appl. Pharmacol.* **142**, 229-242.

Baranano, D. E., Ferris, C. D. and Snyder, S. H. (2001). Atypical neural messengers. *Trends Neurosci.* **24**, 99-106.

Bellocchio, E. E., Hu, H., Pohorille, A., Chan, J., Pickel, V. M. and Edwards, R. H. (1998). The localization of the brain-specific inorganic phosphate transporter suggests a specific presynaptic role in glutamatergic transmission. *J. Neurosci.* **18**, 8648-8659.

Bellocchio, E. E., Reimer, R. J., Fremeau, R. T., Jr and Edwards, R. H. (2000). Uptake of glutamate into synaptic vesicles by an inorganic phosphate transporter. *Science* **289**, 957-960.

Bonifacino, J. S. and Traub, L. M. (2003). Signals for sorting of transmembrane proteins to endosomes and lysosomes. *Annu. Rev. Biochem.* **72**, 395-447.

Bramham, C. R., Torp, R., Zhang, N., Storm-Mathisen, J. and Ottersen, O. P. (1990). Distribution of glutamate-like immunoreactivity in excitatory hippocampal pathways: a semiquantitative electron microscopic study in rats. *Neuroscience* **39**, 405-417.

Chao, Y. and Fu, D. (2004). Kinetic study of the antiport mechanism of an *Escherichia coli* zinc transporter, ZitB. *J. Biol. Chem.* **279**, 17173-17180.

Cole, T. B., Wenzel, H. J., Kafer, K. E., Schwartzkroin, P. A. and Palmiter, R. D. (1999). Elimination of zinc from synaptic vesicles in the intact mouse brain by disruption of the ZnT3 gene. *Proc. Natl. Acad. Sci. USA* **96**, 1716-1721.

Cole, T. B., Robbins, C. A., Wenzel, H. J., Schwartzkroin, P. A. and Palmiter, R. D. (2000). Seizures and neuronal damage in mice lacking vesicular zinc. *Epilepsy Res.* **39**, 153-169.

Colvin, R. A., Davis, N., Nipper, R. W. and Carter, P. A. (2000a). Evidence for a zinc/proton antiporter in rat brain. *Neurochem. Int.* **36**, 539-547.

Colvin, R. A., Davis, N., Nipper, R. W. and Carter, P. A. (2000b). Zinc transport in the brain: routes of zinc influx and efflux in neurons. *J. Nutr.* **130**, 1484S-1487S.

de Wit, H., Lichtenstein, Y., Geuze, H., Kelly, R. B., van der Sluijs, P. and Klumperman, J. (1999). Synaptic vesicles form by budding from tubular extensions of sorting endosomes in PC12 cells. *Mol. Biol. Cell* **10**, 4163-4176.

Faundez, V. V. and Kelly, R. B. (2000). The AP-3 complex required for endosomal synaptic vesicle biogenesis is associated with a casein kinase Ialpha-like isoform. *Mol. Biol. Cell* **11**, 2591-2604.

Faundez, V., Horng, J. T. and Kelly, R. B. (1997). ADP ribosylation factor 1 is required for synaptic vesicle budding in PC12 cells. *J. Cell Biol.* **138**, 505-515.

Faundez, V., Horng, J. T. and Kelly, R. B. (1998). A function for the AP3 coat complex in synaptic vesicle formation from endosomes. *Cell* **93**, 423-432.

Geffard, M., Buijs, R. M., Seguela, P., Pool, C. W. and le Moal, M. (1984). First demonstration of highly specific and sensitive antibodies against dopamine. *Brain Res.* **294**, 161-165.

Gouras, G. K. and Beal, M. F. (2001). Metal chelator decreases Alzheimer beta-amyloid plaques. *Neuron* **30**, 641-642.

Grote, E., Hao, J. C., Bennett, M. K. and Kelly, R. B. (1995). A targeting signal in VAMP regulating transport to synaptic vesicles. *Cell* **81**, 581-589.

Huang, E. P. (1997). Metal ions and synaptic transmission: think zinc. *Proc. Natl. Acad. Sci. USA* **94**, 13386-13387.

Kantheti, P., Qiao, X., Diaz, M. E., Peden, A. A., Meyer, G. E., Carskadon, S. L., Kapfhamer, D., Sufalko, D., Robinson, M. S., Noebels, J. L. et al. (1998). Mutation in AP-3 delta in the mocha mouse links endosomal transport to storage deficiency in platelets, melanosomes, and synaptic vesicles. *Neuron* **21**, 111-122.

Kantheti, P., Diaz, M. E., Peden, A. E., Seong, E. E., Dolan, D. F., Robinson, M. S., Noebels, J. L. and Burmeister, M. L. (2003). Genetic and phenotypic analysis of the mouse mutant *mh(2J)*, an *Ap3d* allele caused by IAP element insertion. *Mamm. Genome* **14**, 157-167.

Lee, J. Y., Cole, T. B., Palmiter, R. D., Suh, S. W. and Koh, J. Y. (2002). Contribution by synaptic zinc to the gender-disparate plaque formation in human Swedish mutant APP transgenic mice. *Proc. Natl. Acad. Sci. USA* **99**, 7705-7710.

Lee, J. Y., Kim, J. H., Hong, S. H., Cherny, R. A., Bush, A. I., Palmiter, R. D. and Koh, J. Y. (2004). Estrogen decreases zinc transporter 3 expression and synaptic vesicle zinc levels in mouse brain. *J. Biol. Chem.* **279**, 8602-8607.

Li, Y., Hough, C. J., Frederickson, C. J. and Sarvey, J. M. (2001). Induction of mossy fiber → CA3 long-term potentiation requires translocation of synaptically released Zn^{2+}. *J. Neurosci.* **21**, 8015-8025.

Lichtenstein, Y., Desnos, C., Faundez, V., Kelly, R. B. and Clift-O'Grady, L. (1998). Vesiculation and sorting from PC12-derived endosomes in vitro. *Proc. Natl. Acad. Sci. USA* **95**, 11223-11228.

Liu, Y. and Edwards, R. H. (1997). Differential localization of vesicular acetylcholine and monoamine transporters in PC12 cells but not CHO cells. *J. Cell Biol.* **139**, 907-916.

Lopantsev, V., Wenzel, H. J., Cole, T. B., Palmiter, R. D. and Schwartzkroin, P. A. (2003). Lack of vesicular zinc in mossy fibers does not affect synaptic excitability of CA3 pyramidal cells in zinc transporter 3 knockout mice. *Neuroscience* **116**, 237-248.

Lu, Y. M., Taverna, F. A., Tu, R., Ackerley, C. A., Wang, Y. T. and Roder, J. (2000). Endogenous Zn(2+) is required for the induction of long-term potentiation at rat hippocampal mossy fiber-CA3 synapses. *Synapse* **38**, 1871-1897.

Naito, S. and Ueda, T. (1985). Characterization of glutamate uptake into synaptic vesicles. *J. Neurochem.* **44**, 99-109.

Nasir, M. S., Fahrni, C. J., Suhy, D. A., Kolodsick, K. J., Singer, C. P. and O'Halloran, T. V. (1999). The chemical cell biology of zinc: structure and intracellular fluorescence of a zinc-quinolinesulfonamide complex. *J. Biol. Inorg. Chem.* **4**, 775-783.

Palmiter, R. D., Cole, T. B., Quaife, C. J. and Findley, S. D. (1996). ZnT-3, a putative transporter of zinc into synaptic vesicles. *Proc. Natl. Acad. Sci. USA* **93**, 14934-14939.

Paoletti, P., Ascher, P. and Neyton, J. (1997). High-affinity zinc inhibition of NMDA NR1-NR2A receptors. *J. Neurosci.* **17**, 5711-5725.

Prekeris, R., Klumperman, J., Chen, Y. A. and Scheller, R. H. (1998). Syntaxin 13 mediates cycling of plasma membrane proteins via tubulovesicular recycling endosomes. *J. Cell Biol.* **143**, 957-971.

Reimer, R. J., Fremeau, R. T., Jr., Bellocchio, E. E. and Edwards, R. H. (2001). The essence of excitation. *Curr. Opin. Cell Biol.* **13**, 417-421.

Robinson, M. S. (2004). Adaptable adaptors for coated vesicles. *Trends Cell Biol.* **14**, 167-174.

Saito, T., Takahashi, K., Nakagawa, N., Hosokawa, T., Kurasaki, M., Yamanoshita, O., Yamamoto, Y., Sasaki, H., Nagashima, K. and Fujita, H. (2000). Deficiencies of hippocampal Zn and ZnT3 accelerate brain aging of rat. *Biochem. Biophys. Res. Commun.* **279**, 505-511.

Salazar, G., Love, R., Styers, M. L., Werner, E., Peden, A., Rodriguez, S., Gearing, M., Wainer, B. H. and Faundez, V. (2004a). AP-3-dependent mechanisms control the targeting of a chloride channel (ClC-3) in neuronal and non-neuronal cells. *J. Biol. Chem.* **279**, 25430-25439.

Salazar, G., Love, R., Werner, E., Doucette, M. M., Cheng, S., Levey, A. and Faundez, V. (2004b). The zinc transporter ZnT3 interacts with AP-3 and it is preferentially targeted to a distinct synaptic vesicle subpopulation. *Mol. Biol. Cell* **15**, 575-587.

Salem, N., Faundez, V., Horng, J. T. and Kelly, R. B. (1998). A v-SNARE participates in synaptic vesicle formation mediated by the AP3 adaptor complex. *Nat. Neurosci.* **1**, 551-556.

Schafer, M. K., Varoqui, H., Defamie, N., Weihe, E. and Erickson, J. D. (2002). Molecular cloning and functional identification of mouse vesicular glutamate transporter 3 and its expression in subsets of novel excitatory neurons. *J. Biol. Chem.* **277**, 50734-50748.

Seong, E., Wainer, B. H., Hughes, E. D., Saunders, T. L., Burmeister, M. and Faundez, V. (2005). Genetic analysis of the neuronal and ubiquitous AP-3 adaptor complexes reveals divergent functions in brain. *Mol. Biol. Cell* **16**, 128-140.

Shi, G., Faundez, V., Roos, J., Dell'Angelica, E. C. and Kelly, R. B. (1998). Neuroendocrine synaptic vesicles are formed in vitro by both

clathrin-dependent and clathrin-independent pathways. *J. Cell Biol.* **143**, 947-955.

Sinakevitch, I., Farris, S. M. and Strausfeld, N. J. (2001). Taurine-, aspartate- and glutamate-like immunoreactivity identifies chemically distinct subdivisions of Kenyon cells in the cockroach mushroom body. *J. Comp. Neurol.* **439**, 352-367.

Somogyi, P., Halasy, K., Somogyi, J., Storm-Mathisen, J. and Ottersen, O. P. (1986). Quantification of immunogold labelling reveals enrichment of glutamate in mossy and parallel fibre terminals in cat cerebellum. *Neuroscience* **19**, 1045-1050.

Storm-Mathisen, J., Leknes, A. K., Bore, A. T., Vaaland, J. L., Edminson, P., Haug, F. M. and Ottersen, O. P. (1983). First visualization of glutamate and GABA in neurones by immunocytochemistry. *Nature* **301**, 517-520.

Storm-Mathisen, J., Ottersen, O. P., Fu-Long, T., Gundersen, V., Laake, J. H. and Nordbo, G. (1986). Metabolism and transport of amino acids studied by immunocytochemistry. *Med. Biol.* **64**, 127-132.

Swedlow, J. R., Sedat, J. W. and Agard, D. A. (1997). Deconvolution in optical microscopy. In *Deconvolution of Images and Spectra* (ed. P. A. Jansson), pp. 284-307. San Diego: Academic Press.

Takamori, S., Rhee, J. S., Rosenmund, C. and Jahn, R. (2000a). Identification of a vesicular glutamate transporter that defines a glutamatergic phenotype in neurons. *Nature* **407**, 189-194.

Takamori, S., Riedel, D. and Jahn, R. (2000b). Immunoisolation of GABA-specific synaptic vesicles defines a functionally distinct subset of synaptic vesicles. *J. Neurosci.* **20**, 4904-4911.

Takeda, A. (2000). Movement of zinc and its functional significance in the brain. *Brain Res. Brain Res. Rev.* **34**, 137-148.

Ueno, S., Tsukamoto, M., Hirano, T., Kikuchi, K., Yamada, M. K., Nishiyama, N., Nagano, T., Matsuki, N. and Ikegaya, Y. (2002). Mossy fiber Zn^{2+} spillover modulates heterosynaptic *N*-methyl-D-aspartate receptor activity in hippocampal CA3 circuits. *J. Cell Biol.* **158**, 215-220.

van de Goor, J., Ramaswami, M. and Kelly, R. (1995). Redistribution of synaptic vesicles and their proteins in temperature-sensitive *shibire(ts1)* mutant *Drosophila*. *Proc. Natl. Acad. Sci. USA* **92**, 5739-5743.

Varoqui, H., Schafer, M. K., Zhu, H., Weihe, E. and Erickson, J. D. (2002). Identification of the differentiation-associated Na^+/PI transporter as a novel vesicular glutamate transporter expressed in a distinct set of glutamatergic synapses. *J. Neurosci.* **22**, 142-155.

Vogt, K., Mellor, J., Tong, G. and Nicoll, R. (2000). The actions of synaptically released zinc at hippocampal mossy fiber synapses. *Neuron* **26**, 187-196.

Weiss, J. H., Sensi, S. L. and Koh, J. Y. (2000). Zn(2+): a novel ionic mediator of neural injury in brain disease. *Trends Pharmacol. Sci.* **21**, 395-401.

Wenzel, H. J., Cole, T. B., Born, D. E., Schwartzkroin, P. A. and Palmiter, R. D. (1997). Ultrastructural localization of zinc transporter-3 (ZnT-3) to synaptic vesicle membranes within mossy fiber boutons in the hippocampus of mouse and monkey. *Proc. Natl. Acad. Sci. USA* **94**, 12676-12681.

Zalewski, P. D., Forbes, I. J. and Betts, W. H. (1993). Correlation of apoptosis with change in intracellular labile Zn(II) using zinquin [(2-methyl-8-*p*-toluenesulphonamido-6-quinolyloxy)acetic acid], a new specific fluorescent probe for Zn(II). *Biochem. J.* **296**, 403-408.

Zhou, Q., Petersen, C. C. and Nicoll, R. A. (2000). Effects of reduced vesicular filling on synaptic transmission in rat hippocampal neurones. *J. Physiol.* **525**, 195-206.

Journal of Cell Science